

EXPERIMENTAL RESEARCH OF AN INTEGRATED SCAVENGING PUMP COUPLED WITH A BUFFER TANK FOR A FREE-PISTON ENGINE

by

Yu LIU, Jinlong WANG, Jin XIAO*, and Zhen HUANG

Key Laboratory of Power Machinery and Engineering, Ministry of Education,
Shanghai Jiao Tong University, Shanghai, China

Original scientific paper
<https://doi.org/10.2298/TSCI240608200L>

Free-piston engine is considered one of the potential range extenders for hybrid vehicles because of its high thermal efficiency, low mechanical loss, and ultimate fuel flexibility. The performance of scavenging devices or structures is critical of two-stroke free-piston engine stable operation. This paper aims to explore the operating characteristics of an integrated scavenging pump coupled with a buffer tank under different operating conditions to promote the application of scavenging pumps on free-piston engines. Hence, a detailed contrast experiment is performed to investigate the effect of the buffer tank volume, discharge position and deflated pressure on the scavenging pump performance. By analysing the experimental results, a weighting score system is employed in deciding the most appropriate buffer tank for the application. The CFD calculation of the gas exchanging process to validate the feasibility of the selected scavenging pump parameters. In addition, the influence of buffer tank pressure on combustion is evaluated via scavenging combustion tests. The experiment results show that the maximum in-cylinder pressure can reach 47.44 bar when the buffer tank pressure 165 kPa.

Key words: *free-piston engine, scavenging pump,
buffer tank, pressure fluctuation*

Introduction

The decarbonization of the transportation sector has been the subject of research for several years, gaining increased attention recently [1]. According to the statistics, 20% of global anthropogenic GHG emissions are derived from the transportation sector [2]. It is commonly acknowledged that the most obvious way to achieve decarbonization is the less use of fossil fuels. Therefore, many technologies for passenger transport decarbonization are presented. One technology that attracts remarkable public attention is free-piston engine generator (FPEG). It is employed as a range extender for hybrid vehicles and considered as one of the promising technologies. The piston of the free-piston engine can move freely without the kinematic constraint of a crankshaft. Therefore, the compression ratio and stroke vary in cycle by cycle. By leveraging this feature, FPEG has the advantages of higher thermal efficiency, less mechanical loss and the capacity for alternative fuels and combustion modes [3].

Researchers from the German Aerospace Center (DLR) had proposed a spark ignited FPEG with an adjustable gas spring that reports a cylinder diameter of 82.5 mm and a maximum

* Corresponding author, e-mail: xiaojin@sjtu.edu.cn

stroke of 90 mm in continuous operation [4, 5]. An electromagnetic valve train system was adapted to realize the required flexibility in valve timing. To investigate the scavenging process of a free-piston engine, laser diagnostic measurements and CFD simulations were performed. It was found that two inlets and one outlet valve were the best options [4]. Moreover, compared with the full load with spark ignition combustion mode, the homogeneous charge compression ignition combustion mode had higher indicated efficiency [6].

Researchers in Toyota Central R&D Labs Inc. presented a single-piston FPEG with a *W*-shaped piston [7-9]. Scavenging was provided through scavenging ports in the cylinder liner and the exhaust valve was installed on the cylinder head [8, 9]. Two control strategies were proposed based on the position feedback control method. The experiment showed that the prototype could successfully operate for more than 4 hours running at 23 Hz with a compression ratio of 14 [7].

Mikalsen and Roskilly [10-12] at Newcastle University had proposed a modular compression ignition FPEG. A turbocharged two-stroke Diesel engine was employed and electronically-controlled exhaust poppet valves were mounted on the cylinder head. They also presented numerical modelling and simulation analysis of a spark-ignition FPEG and a compression-ignition FPEG, respectively. The simulation result showed that the parameters of the FPEG had highly coupled and non-linear performance. In addition, the frictional loss and NO_x emission was lower than that of TRE.

The group of Zhengxing Zuo from Beijing Institute of Technology designed a compression-ignition FPEG with diesel as fuel. The prototype utilized an air blower to supply fresh gas for the engine to achieve good scavenging performance [13, 14]. They also proposed a parameter coupling method for diesel free-piston-linear alternator. The CFD and 0-D numerical simulation were employed to optimize the geometric parameters of the two-stroke engine. The results showed that the free-piston-engine alternator with the best parameters can operate in good scavenging performance [15].

Pempek Systems company designed a prototype of the free-piston power pack (FP3) in 2003. The prototype had an extremely compact structure, with an integral compressor and a passive intake valve located in the head of the piston. Two-stroke engine was applied to the FP3 with SI combustion mode. The FP3 could produce 40 kW at an operating frequency 30.4 Hz and increase the output power by adjusting the size and number of FP3 modules [16].

Nanjing University of Science and Technology had developed a single-cylinder FPEG prototype. The prototype utilized a piston compress the air in the scavenging chamber to scavenge exhaust gas. In order to enable stable operating, a reciprocating motion control strategy was proposed. The test results showed that the prototype could achieve stable reciprocating motion, but the bottom turning center position had a certain deviation [17].

The performance of scavenging devices or structures is critical of two-stroke engine stable operation [18]. Compared with the traditional two-stroke internal combustion engine, the two-stroke free-piston engine has to utilize the devices or structures to scavenge exhaust gas due to lack of crankcase. The apparatus or structures in existing research proposed to scavenge the burned gas for two-stroke free-piston engine can be included in three categories:

- External equipment- employ fan, compressor, turbocharger, or other devices [12, 14, 19]. It can provide all kinds of demand of scavenging air pressure, and the disadvantage is larger volume and higher cost [16].
- Exhaust valves- excellent exhaust emissions performance and was driven by mechanical, electro-hydraulic, motor-driven or electromechanical [6, 20, 21]. The devices have a complex structure or are difficult to control [22].

- Self-structure- compact structure, scavenge air pressure have large variation due to absence of buffer device and cannot effectively be controlled [17, 23].

Currently there is little research that has presented the explore of scavenging devices or structures which employed in FPEG. They mainly focus on the scavenging process or main geometric dimensions of the two-stroke free-piston engine. To improve scavenging efficiency and achieve stable operation FPEG, the operating characteristics of a scavenging device should be researched initially. Therefore, an integrated scavenging pump is proposed and analyzed in this research. The scavenging pumps have simple structure and are easy to control. They can obtain various scavenging pressure. The pressure fluctuation (PF) can be reduced through coupling with a buffer tank. This paper attempts to explore the operating characteristics of an integrated scavenging pump coupled with a buffer tank under different operating conditions to promote the application of scavenging pumps on free-piston engine. For this purpose, a detailed contrast experiment is performed to investigate the effect of the buffer tank volume, discharge position and deflated pressure on the scavenging pump performance. By analyzing the experimental results, a weighting score system is employed in deciding the most appropriate buffer tank for the application. The CFD calculation of the gas exchanging process works to validate the feasibility of the scavenging pump. Finally, the influence of buffer tank pressure on combustion is evaluated via scavenging combustion tests.

Experimental set-up

An integrated scavenging pump employed in FPEG

Figure 1 shows the schematic diagram and prototype of FPEG. The main parts of the FPEG system include a two-stroke gasoline engine, a linear permanent magnet synchronous machine (LPMSM) and an integrated scavenging pump. The two-stroke gasoline engine adopts in-cylinder direct injection, spark plug ignition, and loop scavenging structure. The scavenging

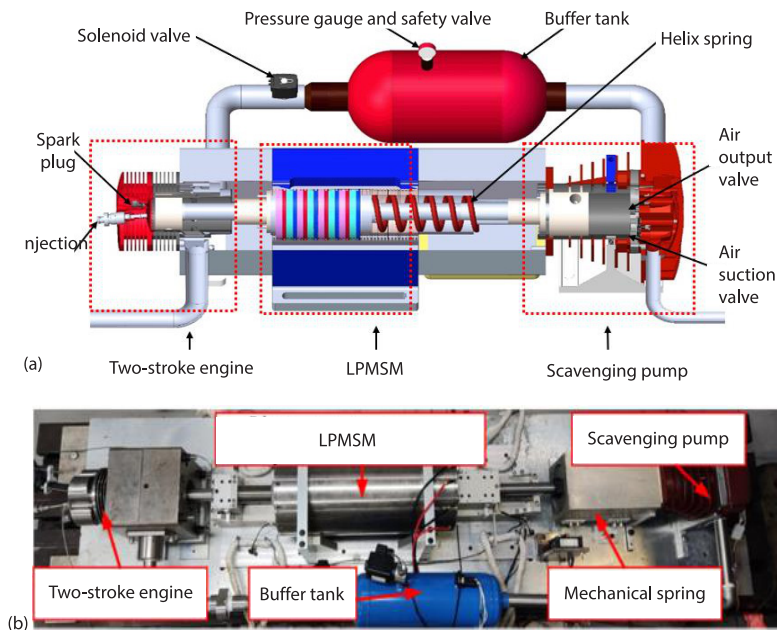


Figure 1. The FPEG system; (a) schematic diagram and (b) prototype and test bench

pump increases the intake air pressure and delivers sufficient fresh charge into the engine's combustion chamber. Specifically, the scavenging pump has two valves: air suction and output. When the piston moves from left to right and the air suction valve is opened passively, the fresh air enters the scavenging pump chamber due to the pressure difference. On the opposite, when the piston moves from right to left and the air output valve is open, the fresh air is compressed and pumped to the engine's combustion chamber. A helix spring is used as the rebound device in the FPEG, and a buffer tank sustain the scavenging pressure level during operation. The control system utilizes NI Compact RIO-9039, a modular high performance embedded controller. The charged scavenging air pressure can be set as 1.5 bar from the previous project [24]. The prototype parameters are listed in tab. 1.

Table 1. Prototype specification

Parameters	Value
Two-stroke engine bore [mm]	70
Scavenging pump bore [mm]	90
Maximum stroke length [mm]	90
Maximum compression ratio	10
Spring elasticity coefficient [Nmm^{-1}]	50

Configuration of scavenging pump test bench

Figure 2 shows the test bench and schematic of the scavenging pump test system. The test system is composed of the test sensors, pipe, scavenging pump, laser displacement sensor, crankshaft, linear motion bearing, rotating motor, frequency converter, buffer tank, bleed valve, solenoid valve, controller and data acquire system. The rotating motor is controlled by a frequency converter. The laser displacement sensor measures the piston position. The bleed valve and solenoid valve were controlled by the NI Compact RIO-9039 which is a modular high performance embedded controller. The bleed valve can adjust the pressure in the buffer tank. The solenoid valve controls the flow of gas from the scavenging pump. The temperature and pressure of the inlet, working chamber, buffer tank and outlet are tested by sensors and obtained by the NI Compact RIO-9039 data acquisition system.

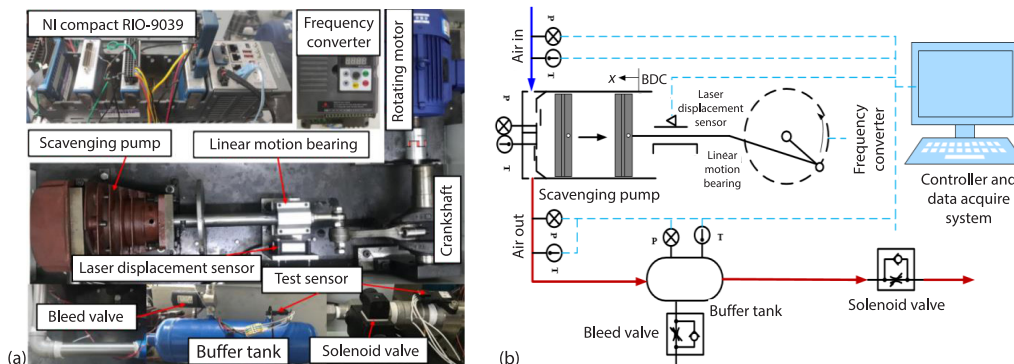


Figure 2. (a) test bench and (b) schematic of scavenging pump test system

Results and discussion

Pressure in the working chamber

Figure 3 shows the experimental data collected as a function of time. In the suction process, the inlet pressure is maintained roughly the value of 95 kPa. The piston begins to move from BDC to TDC in the compression process, and the pressure gradually increases. The air output valve is open when the scavenging air is pumped to discharge pressure. The scavenging pump starts the delivery phase. Air is continuously pushed out from the scavenging pump around 150 kPa. The delivery phase ends when the scavenging piston reaches the TDC point, and then the expansion phase starts. During this process, the pressure in the scavenging chamber is reduced while the piston moves towards the BDC. Such a pressure reduction continues till the chamber pressure becomes the ambient pressure. Afterward, the scavenging pump goes into the suction phase, while the in-cylinder air pressure is lower than ambient pressure. Then the compression phase starts again and forms an operation cycle of the scavenging pump.

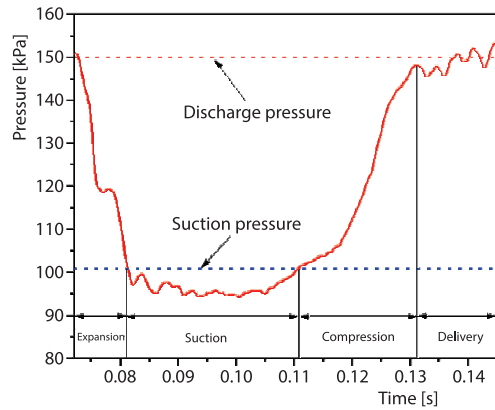


Figure 3. Experimental diagram of the working cycle

Effect of buffer tank

Figure 4 shows the pressures curves with and without buffer tank conditions. The relative amplitude of the pulsation pressure can be calculated:

$$PF = \frac{P_{\max} - P_{\min}}{P_{\text{mean}}} \times 100\% \quad (1)$$

where P_{\max} and P_{\min} are the maximum and the minimum value of the pressure wave profile in one period under stable running operating points. The P_{mean} can be obtained by an integral mean method.

As shown in fig. 4(a), the PF without buffer tank ($PF = 69.15\%$) is obviously greater than buffer tank conditions ($PF = 24.34\%$) under stable running operating point. Figure 4(b) provides the pressure curves under piston operating frequency 12 Hz with the bleed valve closed. It can be seen that the mean pressure is 173.59 kPa more than the requirement of 150 kPa. Therefore, the bleed valve is required to be opened to obtain a discharge pressure 150 kPa. As figs. 4(c) and 4(d) reveal, whether the bleed valve is open or closed, the buffer tank always has the role of reducing the pulsation of air explicitly and ensuring the fresh air enters the two-stroke engine smoothly.

Figure 5 presents the pressure pulsation in the buffer tank. As shown in fig. 5, the pressure in the buffer tank maintains roughly the fixed value of 162 kPa (1-2), and then increases with the increasing of displacement (2-3) because of compression progress, and then fluctuates around 174.28 kPa (3-4), finally decrease with the decreasing of displacement (4-1) due to solenoid valve being opened. Figure 6 compares the PF in different volumes of buffer tanks with various frequencies. The mean pressure in the buffer tank increase with increasing piston frequency and buffer tank volume under bleed closed and solenoid valve opened position 44.5 mm conditions. The target pressure 150 kPa has been obtained in frequency 10 Hz. Moreover, the PF decreases with an increase in the volume of the buffer tank and has little influence by

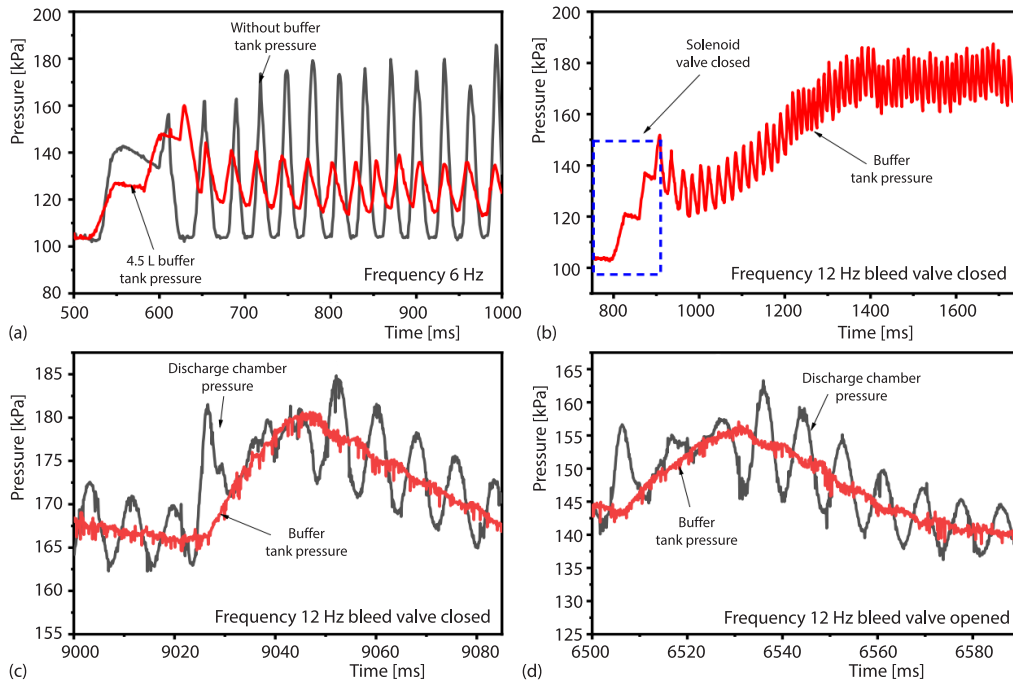


Figure 4. Pressures curves under without and with buffer tank conditions

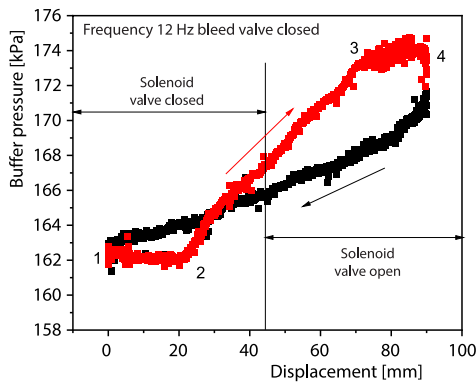


Figure 5. Pressure pulsation in buffer tank

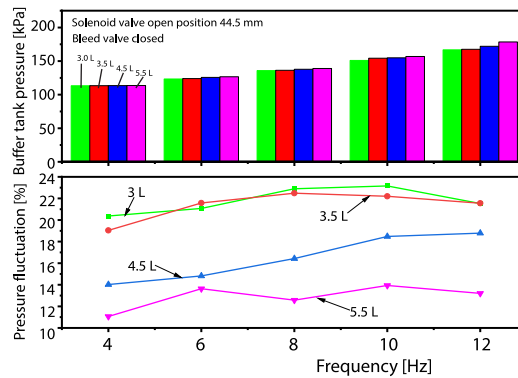


Figure 6. Pressure pulsation in buffer tank

frequency. It can be attributed to two aspects: scavenging pump completes more cycles in a given amount of time and a higher percentage (discharge volume ratio the buffer tank volume) in smaller buffer tank volume.

Figure 7 shows the changing of the number of cycles before 1st solenoid valve opened under different buffer tank volumes as frequency changes. It can be seen in fig. 7 that the larger volume of the buffer tank, the more cycles are required. The number of cycles for buffer tank volumes 3 L, 3.5 L, 4.5 L, and 5.5 L is 1.5, 2.25, 2.5, and 3.5, respectively. The number of cycles can represent the energy consumed by the motor. Therefore, the larger the buffer tank volume, the more energy motor consumes before 1st solenoid valve is opened.

Effect of discharge position and deflated pressure

The discharge position refers to the initial position of the piston when the solenoid valve is opened. Figure 8 presents a comparison of the pressure and PF in different discharge position 36 mm (engine exhaust port opened), 44.5 mm (the middle of exhaust port and intake port) and 53 mm (engine intake port opened) with various frequency. The results indicate that the mean pressure in buffer tank significantly increased with increasing piston frequency and discharge position under bleed valve closed conditions. It is because of that the discharge position represents the time of pressure accumulation in buffer tank. The earlier the solenoid valve opens, the less pressure builds in the buffer tank. The PF increased with the increase of discharge position.

The deflated pressure is the control signal to open the bleed valve. The bleed valve is opened when the pressure in the buffer tank is greater than the deflated pressure. The buffer tank pressure and PF with the deflated pressure are recorded and depicted in fig. 9. It can be seen that the pressure of the buffer tank increases when the deflated pressure increases. The PF is almost immune to the deflated pressure. Moreover, buffer tank pressure rises with the buffer tank volume increases. The reason is that the solenoid valve has a time delay in closing. When the value of time delay is the same, the smaller volume buffer tank, the higher percentage (leaked gas volume over the buffer tank volume) and the lower the pressure. The leaked gas also represents energy loss. Therefore, it is a requirement to obtain target pressure with lower energy loss.

Weighting criteria

A weighting score system is employed in deciding the most appropriate buffer tank for the application. The final score of both buffer tanks is to judge the selection of the appropriate topology for the desired application. The authors take into consideration the number of cycles 1st solenoid valve open (evaluating based on 5), pressure pulsation (evaluating based on 25%) and deflated pressure (evaluating based on 150 kPa), decide the percentage score used. The buffer tank is used to reduce PF. Therefore, the weight of PF is greater than energy consump-

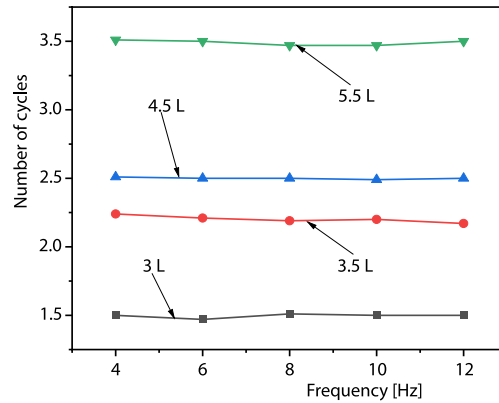


Figure 7. Number of cycles before 1st solenoid valve open

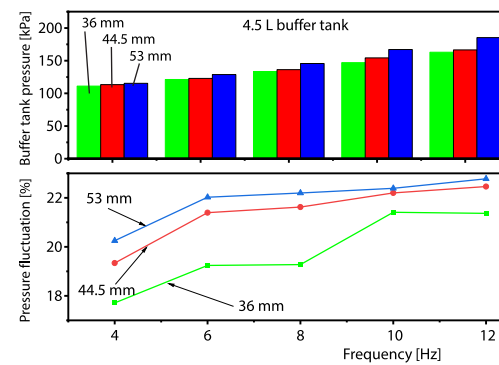


Figure 8. The changing of the buffer tank pressure under different discharge position

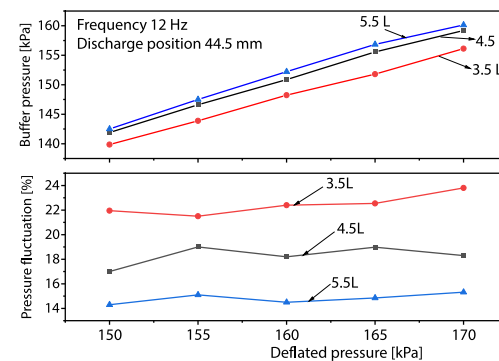


Figure 9. The pressure of buffer tank and PF at different deflated pressure

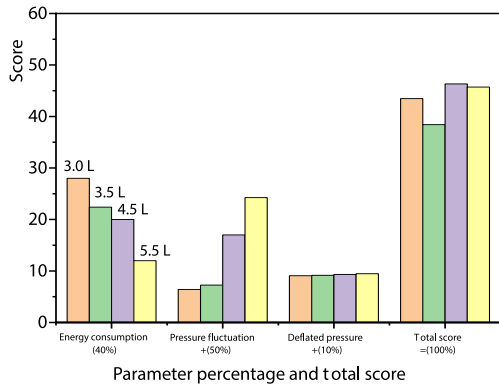


Figure 10. Scoring system results

tion (represented by the number of cycles) and energy loss (represented by deflated pressure). Considering that the first build-up of the buffer tank pressure requires more motor energy, energy consumption weight is greater than energy loss. Figure 10 shows the results of the scoring system application. The 4.5 L buffer tank score is obviously higher than that of the other volume buffer tank.

Figure 11 illustrates the variation of the mean pressure in high piston operating frequency under a 4.5 L buffer tank. According to fig. 11(a) that there is a slight difference in the pressure of the buffer tank with the condition of discharge position 44.5 mm and deflated pressure 160 kPa. Moreover, the pulsation pressure is about 18.91% in frequency 30 Hz, as shown in fig. 11(b). Thus, based on the scoring system and results at 18-30 Hz, the 4.5 L buffer tank is more comfortable for this application.

Figure 11 illustrates the variation of the mean pressure in high piston operating frequency under a 4.5 L buffer tank. According to fig. 11(a) that there is a slight difference in the pressure of the buffer tank with the condition of discharge position 44.5 mm and deflated pressure 160 kPa. Moreover, the pulsation pressure is about 18.91% in frequency 30 Hz, as shown in fig. 11(b). Thus, based on the scoring system and results at 18-30 Hz, the 4.5 L buffer tank is more comfortable for this application.

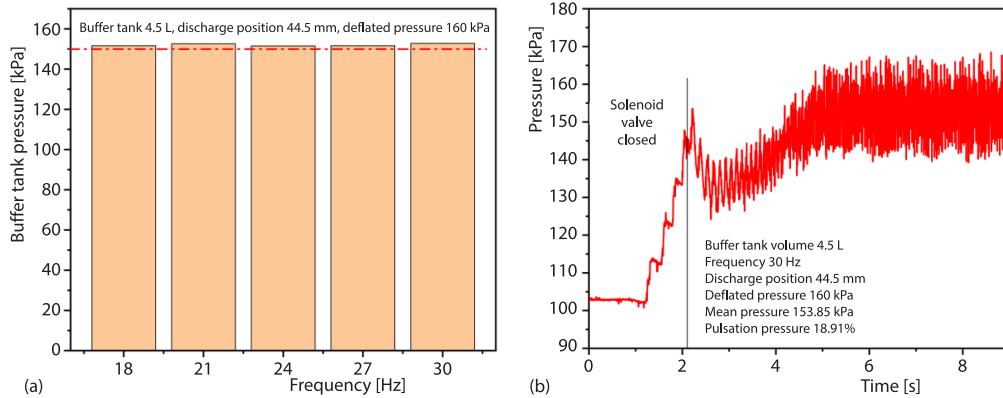


Figure 11. The buffer tank pressure in high frequency

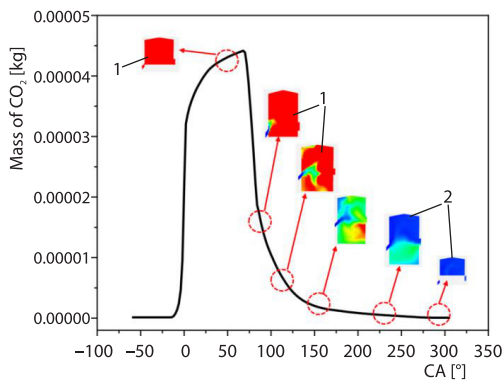


Figure 12. The mass of CO₂ vs. virtual CA during gas exchanging process

Gas exchanging process

To validate the feasibility of the scavenging pump, the test data of frequency 30 Hz and virtual crankshaft are selected to study CFD calculation of the gas exchanging process. The test data of frequency 30 Hz is introduced into the CONVERAGE CFD 3-D simulation. As a typical combustion product, CO₂ can characterize the degree of ventilation in the cylinder and the mass of CO₂ during the gas exchanging process are shown in fig. 12. As shown in fig. 12, the mass of CO₂ decreases from 44.2 mg to approach zero, the combustion chamber

is initially filled with burn gases (red color – 1) and the scavenging pump system provide fresh air (blue color – 2). At the end of the gas exchanging process, fresh air fills the cylinder, and the burned gas has been scavenged out of the cylinder with the scavenging efficiency 97.96%.

Scavenging combustion tests

For the sake of obtaining the influence of buffer tank pressure on FPEG system, FPEG test bench is utilized to conduct the operation experiment, as shown in fig. 1. The fuel injection mass is 20 mg per cycle and is injected in the combustion chamber when the exhaust port just closed. The spark timing is first set as the time when the piston reaches 88 mm.

The experiment results are shown in fig. 13. It is found that the maximum in-cylinder pressure starts to increase and then decreases when the buffer tank pressure continues to rise. When the buffer tank pressure 165 kPa, the maximum in-cylinder pressure achieves 47.44 bar. This is due to that there is more fresh air in the combustion chamber and the exhaust is effectively removed during scavenging. The decrease is owing to the decrease in compression ratio. In the prototype test bench, the buffer tank is connected to the combustion chamber by the pipe. The pressure drop occurs during the fresh air-flow from the buffer tank to free-piston engine. The pressure losses are caused by frictional losses within the pipe and 90° elbow. Therefore, the buffer tank pressure should be above 150 kPa to offset pressure loss during pipe transportation.

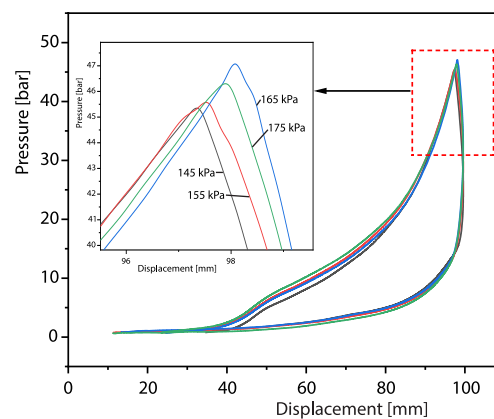


Figure 13. Experiment results of pressure in the combustion chamber with different buffer tank

Conclusions

In this paper, a contrast experiment is carried out to investigate the effect of the buffer tank volume, discharge position and deflated pressure on the scavenging pump performance. The conclusions are as follows.

- The buffer tank always has the role of explicitly reducing the pulsation of air no matter whether the bleed valve is open or closed. The more buffer tank volume, the less PF. This means that the engine can be provided with a stable sweep pressure and more fresh air, creating the conditions for fuel combustion. It can improve the scavenging efficiency of the engine. However, a larger volume buffer tank increases the number of cycles before the prescribed pressure level is reached. It means that more energies are supplied by the motor.
- The earlier the solenoid valve opens, the less time of pressure accumulation and the less pressure builds in the buffer tank. The PF increases with the increase of discharge position and is almost immune to the deflated pressure. When the deflated pressure is constant, buffer tank pressure increases with the buffer tank volume increases. The proper deflated pressure should be selected to reduce energy loss.
- The comparison made via the suggested scoring system showed that the 4.5 L buffer tank is more comfortable for this application, even in high frequency. The mean pressure is 153.85 kPa and the pulsation pressure is about 18.91% in frequency 30Hz.

- The CFD calculation of the gas exchanging process results demonstrated the very good efficiency of the scavenging process. The pressure drop occurs during pipe transportation. When the buffer tank pressure 165 kPa, the maximum in-cylinder pressure achieves 47.44 bar. It is necessary to increase the buffer tank pressure properly to obtain 1.5bar scavenging pressure in the position of the engine inlet.

Acknowledgment

This project is supported by the project of Science and Technology Commission of Shanghai Municipality (19511108500). We would like to thank the sponsors.

References

- [1] Kazi, M.-K., et al., Green Hydrogen For Industrial Sector Decarbonization: Costs and Impacts on Hydrogen Economy in Qatar, *Comput. Chem. Eng.*, 145 (2021), 107144
- [2] Dillman, K., et al., Decarbonization Scenarios for Reykjavik's Passenger Transport: The Combined Effects of Behavioural Changes and Technological Developments, *Sustain., Cities Soc.*, 65 (2021), 102614.
- [3] Zhou, Y., et al., A System-Level Numerical Study of a Homogeneous Charge Compression Ignition Spring-Assisted Free Piston-Linear Alternator with Various Piston Motion Profiles, *Applied Energy*, 239 (2019), Apr., pp. 820-35
- [4] Haag, J., et al., Numerical and Experimental Investigation of in-Cylinder Flow in a Loop-Scavenged Two-Stroke Free Piston Engine, SAE Technical Paper, 2013-24-0047, 2013
- [5] Kock, F., et al., The Free Piston-Linear Generator-Development of an Innovative, Compact, Highly Efficient Range-Extender Module, SAE Technical Paper, 2013-01-1727, 2013
- [6] Haag, J., et al., Development Approach for the Investigation of Homogeneous Charge Compression Ignition in a Free-Piston Engine, SAE Technical Paper, 2013-24-0047, 2013
- [7] Kosaka, H., et al., Development of Free Piston Engine Linear Generator System Part 1 – Investigation of Fundamental Characteristics, SAE Technical Paper, 2014-01-1203, 2014
- [8] Goto, S., et al., Development of Free Piston Engine Linear Generator System Part 2 – Investigation of Control System for Generator, SAE Technical Paper, 2014-01-1193, 2014
- [9] Moriya, K., et al., Development of Free Piston Engine Linear Generator System Part 3 – Novel Control Method of Linear Generator for to Improve Efficiency and Stability, SAE Technical Paper, 2016-01-0685, 2016
- [10] Mikalsen, R., Roskilly, A., Coupled Dynamic–Multidimensional Modelling of Free-Piston Engine Combustion, *Applied Engineering*, 86 (2009), 1, pp. 89-95
- [11] Mikalsen, R., Roskilly, A., Performance Simulation of a Spark Ignited Free-Piston Engine Generator, *Applied Thermal Engineering*, 28 (2008), 14-15, pp. 1726-33
- [12] Mikalsen, R., Roskilly, A., The Design and Simulation of a Two-Stroke Free-Piston Compression Ignition Engine for Electrical Power Generation, *Applied Thermal Engineering*, 28 (2008), 5-6, pp. 589-600
- [13] Feng, H., et al., Study of the Injection Control Strategies of a Compression Ignition free Piston Engine Linear Generator in a One-Stroke Starting Process, *Energies*, 9 (2016), 6, 453
- [14] Zhang, Z., et al., Research on the Engine Combustion Characteristics of a Free-Piston Diesel Engine Linear Generator, *Energy Conversion and Management*, 168 (2018), July, pp. 629-38
- [15] Mao, J., et al., Parameters Coupling Designation of Diesel Free-Piston-Linear Alternator, *Applied Energy*, 88 (2011), 12, pp. 4577-89
- [16] Carter, D., Wechner, E., The Free Piston Power Pack: Sustainable Power for Hybrid Electric Vehicles, SAE Technical Paper, 2003-01-3277, 2003
- [17] Yan H, et al., A Reciprocating Motion Control Strategy of Single-Cylinder Free-Piston Engine Generator, *Electronics*, 9 (2020), 2, 245
- [18] Mao, J., et al., Multi-Dimensional Scavenging Analysis of a Free-Piston-Linear Alternator Based on Numerical Simulation, *Applied Energy*, 88 (2011), 4, pp. 1140-1152
- [19] Ismael, M. A., et al., Effect of Aspect Ratio on Frequency And Power Generation of a Free-Piston-Linear Generator, *Applied Thermal Engineering*, 192 (2021), 116944
- [20] Chiang, C.-J., et al., Dynamic Modelling of a SI/HCCI free-Piston Engine Generator with Electric Mechanical Valves, *Applied Energy*, 102 (2013), Feb., pp. 336-46
- [21] Yuan, S., et al., Simulation Study of a Two-Stroke Single Piston Hydraulic Free Piston Engine, 2008 Asia Simulation Conference, *Proceedings*, 7th International Conference on System Simulation and Scientific Computing, Beijing, China, 2008

- [22] Giglio, V., *et al.* Analysis of Advantages and of Problems of Electromechanical Valve Actuators, *SAE Transactions, 111* (2002), Section 3, pp. 1768-1779
- [23] Jia, B., *et al.*, A Decoupled Design Parameter Analysis for Free-Piston Engine Generators, *Energies, 10* (2017), 4, 486
- [24] Zhu, C., Research on Single-Piston Free Piston-Linear Generator System (in Chinese), M. Sc. thesis, Shanghai Jiao Tong University, Shanghai, China, 2019